Phase diagram of D_2 adsorbed on graphene and graphite

C. Carbonell-Coronado and M. C. Gordillo
Departamento de Sistemas Físicos, Químicos y Naturales, Facultad de Ciencias Experimentales, Universidad Pablo de Olavide, Carretera de Utrera, km 1, 41013 Sevilla, Spain
(Received 11 January 2012; revised manuscript received 16 March 2012; published 12 April 2012)

The phase diagram of o-D_2 adsorbed on top of both graphene and graphite was calculated for $T = 0$ K using the diffusion Monte Carlo technique. Both diagrams were found to be virtually identical, except for the energy offset due to the presence of additional graphene sheets in graphite. The ground state of D_2 on graphene and graphite was a $\sqrt{3} \times \sqrt{3}$ commensurate structure that upon a pressure increase was transformed into a so-called γ phase, characterized by an oblique unit cell rotated a given angle with respect to the axis of the upper graphene sheet. At even higher densities, a triangular incommensurate structure similar to the one in the H_2 case is found. A δ commensurate phase at 0.0789 Å^{-2} can barely be distinguished from the γ incommensurate solid at this density, but an ϵ commensurate structure at 0.0835 Å^{-2} is more stable than its γ counterpart. Between the $\sqrt{3} \times \sqrt{3}$ structure and the γ solid, a striped domain wall α phase was found to be more stable than a mixture of both.

DOI: 10.1103/PhysRevB.85.155427 PACS number(s): 67.80.F−, 05.30.Jp

I. INTRODUCTION

The adsorption of different gases on top of graphite is a venerable physics topic from both the experimental and theoretical points of view (see, for instance, Ref. 1 and references therein). In general, we can say that if the temperature is low enough, all gases condense to form a solid monolayer on top of this structure. In the case of ^{4}He and H_2, experimental and theoretical work indicates that their ground states are $\sqrt{3} \times \sqrt{3}$ registered structures.[2–9] The same seems to be true for graphene, a novel form of carbon[10–12] formed by a single isolated carbon sheet similar to those that constitute graphite. For this structure there are no experiments of adsorption yet, but computer simulations[8,9] indicate that the phase diagrams for these two quantum species are very similar in graphene and graphite, the only difference being the binding energies of each particle with the substrate, which are bigger in the case of graphite due to the presence of several graphene layers instead of a single one.

Experimental data on the absorption of D_2 on graphite indicate also a solid $\sqrt{3} \times \sqrt{3}$ ground state,[6,7,13] but instead of having a single phase transition to an incommensurate triangular structure at higher densities, up to four other solid phases were detected in calorimetric studies[7,13] and in neutron[6,14] and electron diffraction experiments.[14,15] From the density corresponding to the $\sqrt{3} \times \sqrt{3}$ structure (0.0636 Å^{-2}) and higher we have a striped domain α phase and two incommensurate structures, a so-called γ phase and a triangular two-dimensional solid of the same type as the one in the H_2 and ^{4}He phase diagrams.[2,7–9] At two definite densities within the stability range of the γ phase, two other commensurate arrangements, a δ phase at 0.0789 Å^{-2} and an ϵ one at 0.0835 Å^{-2}, were found. The existence of these two solids was inferred from calorimetric measurements, but it was not detected in the neutron or electron diffraction experiments. Our goal in this work is to calculate the entire phase diagram of o-D_2 (the rotational ground state of the molecule, a boson) on graphite and graphene and compare our results to the experimental ones.

The plan of this work is as follows. In the next section we describe the computational method used in our calculations, indicating all the parameters and auxiliary hypotheses necessary to carry out the simulations. Section III is devoted to the results obtained, both for the unstable liquids in graphene and graphite and for the stable solid phases of D_2 on both substrates. The last section presents our conclusions.

II. METHOD

The diffusion Monte Carlo (DMC) technique is a numerical algorithm that allows us to obtain the ground state of any bosonic arrangement within some statistical uncertainties.[16] This means that it should give an accurate description of a system of o-D_2 molecules since those particles are bosons. In this work, the D_2 molecules rest on top of a graphene sheet, which was modeled by a set of carbon atoms located in the nodes of a honeycomb lattice. For each D_2 molecule, all the C-D_2 individual contributions to the external potential were taken into account. This potential was taken from Ref. 17 and was previously used to study the behavior of the hydrogen isotopes adsorbed in carbon nanotubes, graphene, and graphite.[9,18,19] In the graphite case, we added also the interactions between each molecule and each carbon atom located on up to the seventh graphene layer below the first one. Those layers were separated a distance of 3.35 Å from each other, as in real graphite, and were stacked in the ABAB fashion that is characteristic of this compound. The inclusion of more carbon sheets did not change the deuterium adsorption energies, something already tested for ^{4}He and H_2 in Refs. 8 and 9. The D_2-D_2 interaction was assumed to be the Silvera and Goldman potential,[22] one of the standards for simulations involving hydrogen isotopes.[18,21]

A fundamental ingredient in the DMC algorithm is the *trial function*, an initial approximation to the real ground-state wave function. The closer this trial function is to the real ground state of the system, the closer the energy obtained by DMC will be to the real one, and the smaller the statistical uncertainties of that energy will be. In this work, we used the following trial

function:

$$\Phi(\mathbf{r}_1,\mathbf{r}_2,\ldots,\mathbf{r}_N) = \prod_{i<j} \exp\left[-\frac{1}{2}\left(\frac{b_{\mathrm{D_2\text{-}D_2}}}{r_{ij}}\right)^5\right] \times \prod_i \prod_J \exp\left[-\frac{1}{2}\left(\frac{b_{\mathrm{C\text{-}D_2}}}{r_{iJ}}\right)^5\right] \times \prod_i \exp[-a(z_i - z_0)^2], \quad (1)$$

i.e., a similar form to the one used in Ref. 9 for H_2 on graphene and graphite. Here, $\mathbf{r}_1,\mathbf{r}_2,\ldots,\mathbf{r}_N$ are the coordinates of the deuterium molecules, and $\mathbf{r}_J$ are the positions of the carbon atoms on each of the graphene layers. This function has several parameters that were optimized variationally. To obtain $b_{\mathrm{C\text{-}D_2}}$, a, and z_0 we performed a series of calculations that included only one D_2 molecule per simulation cell. The minimum energy of this arrangement corresponded to $b_{\mathrm{C\text{-}D_2}} = 2.3$ Å, $a = 5.2$ Å^{-2}, and $z_0 = 2.9$ Å. We used those values for the all the many-body simulations performed in this work. The remaining parameter, $b_{\mathrm{D_2\text{-}D_2}}$, was computed for a system with ten deuterium molecules on a graphene simulation cell of dimensions 34.43×34.08 Å^2, corresponding to 14×8 carbon hexagons. Periodic boundary conditions were used only for the x and y directions. No limits were imposed in the z axis since the deuterium molecules remain always close to the carbon sheets. The optimal value for the $b_{\mathrm{D_2\text{-}D_2}}$ was 3.195 Å. We also kept this parameter fixed for the rest of the simulations with both liquid and solid phases. The same parameters were used for graphite.

However, if we consider solid phases, Eq. (1) is not enough to give an accurate description of the system; it should be multiplied by

$$\prod_i \exp[-c(x_i - x_{\mathrm{site}})^2 - c(y_i - y_{\mathrm{site}})^2], \quad (2)$$

where c is another parameter to be obtained variationally, which, in general, depends on the kind of solid phase we are considering and on the density of that phase. The effect of Eq. (2) on the complete trial function is to limit the range of positions of each particle to a region around its corresponding crystallographic position, $x_{\mathrm{site}}, y_{\mathrm{site}}$. In Table I we display the different parameters obtained for the phases considered in this work. There are only two exceptions: the triangular incommensurate solid found at high pressures and an oblique phase (the so-called γ phase) found at intermediate densities. For the first one, a linear fit between the values obtained at densities of 0.11 Å^{-2} ($c = 2.93$ Å^{-2}) and 0.08 Å^{-2} ($c = 1.11$ Å^{-2}) was used. Below the latter density, c was kept fixed to 1.11 Å^{-2}. The optimal value of c for the γ phase was found to be the same as that for the ϵ phase (see Table I) for the entire density range in which this arrangement was stable.

TABLE I. The c parameters in Eq. (2) variationally obtained for most of the solids considered in this work. For the rest, see the text. For the striped domain phase α, the subindex indicates the number of molecules in their simulation cells. In all cases the error bars were 0.002 Å^{-2}.

Solid phase	c (Å^{-2})
$\sqrt{3} \times \sqrt{3}$	0.459
δ	1.041
ϵ	1.195
γ	1.195
α_4	0.984
α_6	0.853
α_8	0.937
α_{10}	0.949
α_{12}	1.027

III. RESULTS

Our first aim in this work was to obtain the ground state of a system of o-D_2 molecules adsorbed on graphene and graphite. To do so, we started by checking if the liquid phases for these systems are really unstable with respect to the corresponding $\sqrt{3} \times \sqrt{3}$ solids, as found experimentally for graphite.[6,7,13] To simulate the liquids, we used as a trial function the translational invariant Eq. (1) and calculated the energies per deuterium molecule $E(\rho)$ as a function of the deuterium density. To change that density, we varied the number of D_2 molecules adsorbed on simulation cells with dimensions of 34.43×34.08 Å^2. The results are displayed in Fig. 1, where we include also the case of D_2 on a double graphene layer for comparison. The lines are least-squares fits of the different data to

$$E(\rho) = E_0 + \alpha(\rho - \rho_0)^2 + \beta(\rho - \rho_0)^3, \quad (3)$$

where ρ_0 and E_0 stand for the density and the energy per particle at each of the minima of the curves, i.e., at zero pressure. Below ρ_0, the homogeneous liquids would be unstable with respect to the formation of patches of D_2 surrounded by empty space. ρ_0 and E_0 are given in Table II for the three substrates considered. We also include in Table II the adsorption energies in the infinite dilution limit $E_{d\infty}$ and the energies per particle for a $\sqrt{3} \times \sqrt{3}$ commensurate (C) solid.

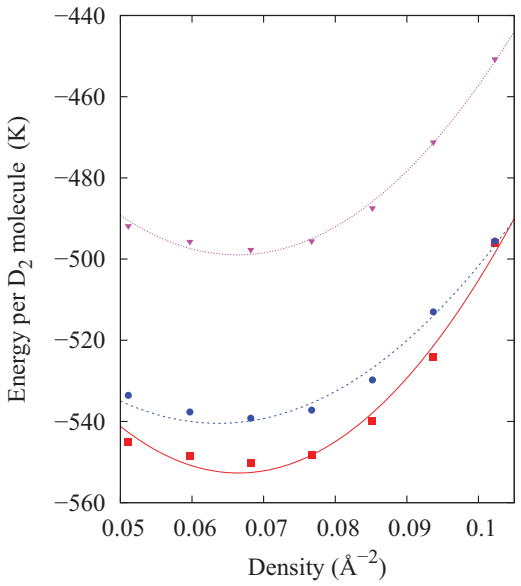

FIG. 1. (Color online) Energy per D_2 molecule (in K) adsorbed on top of graphite (squares), a double graphene layer (circles), and graphene (triangles) as a function of deuterium density. The lines are least-squares fits to Eq. (3) for each system.

TABLE II. Energies per particle and densities at the minima of the curves displayed in Fig. 1, obtained from Eq. (3). Also shown are the energies in the infinite dilution limit $E_{d\infty}$ and the adsorption energies at those minima in relation to that limit. In the last column, we give the energy per deuterium molecule for a $\sqrt{3} \times \sqrt{3}$ registered solid with a density of 0.0636 Å^{-2}.

	E_0 (K)	ρ_0 (Å^{-2})	$E_{d\infty}$ (K)	$(E_0 - E_{d\infty})$ (K)	$E_{(\sqrt{3}\times\sqrt{3})}$ (K)
Graphene	-497.2 ± 0.9	0.064 ± 0.001	-464.87 ± 0.06	-32.3 ± 0.9	-508.533 ± 0.007
Double graphene layer	-539.2 ± 0.9	0.063 ± 0.001	-506.80 ± 0.06	-32.4 ± 0.9	-550.814 ± 0.009
Graphite	-550.9 ± 0.8	0.066 ± 0.001	-517.69 ± 0.05	-33.2 ± 0.8	-561.924 ± 0.008

From the data in Table II we can readily deduce that the $\sqrt{3} \times \sqrt{3}$ arrangement is more stable than a liquid of any density adsorbed on the same substrate. The solids have adsorption energies per particle that are ∼11.5 K lower than the minimum energies of their corresponding liquids. We can also see that the main effect of adding graphene layers is to increase the binding energy an amount that is basically constant for all densities. For instance, in the infinite dilution limit the offset in the adsorption energy between graphene and graphite is 52.82 ± 0.09 K versus 54 ± 1 K for the minima in the liquid vs density curves and 53.39 ± 0.01 K for both $\sqrt{3} \times \sqrt{3}$ structures. The same happens for the pair graphene-double graphene layer, with discrepancies in the range 42 ± 1 K for all phases and densities. It is also interesting to note that the best part of the deuterium-graphite interaction is due to the first two layers since the difference in the deuterium binding energies for the double-graphene structure and graphite is ∼80% of the difference between the interaction between graphene and graphite. In addition, we can also see that the influence of the substrates on the equation of state of the liquid is almost negligible: the adsorption energies $(E_0 - E_{d\infty})$ are within each other's error bars for all the substrates considered, and the same happens with the equilibrium densities, which are all around 0.064 Å^{-2}. These densities are very close to the corresponding C solid one (0.0636 Å^{-2}) and are greater than the ones for the H_2 liquids (around 0.0594 Å^{-2}). Since the only difference between the calculations in this work and those of Ref. 9 is the mass of D_2 versus the mass of H_2, it is obvious that these discrepancies are due to the more classical nature of the former molecule. That is also the cause of the higher adsorption energies for deuterium: -461.12 ± 0.01 and -512.97 ± 0.02 K for the C solid on graphene and graphite[9] (H_2) compared to -508.533 ± 0.007 and -561.924 ± 0.008 K (D_2) from Table II. Those bigger equilibrium densities and binding energies are in line with the simulation results in quasi-one-dimensional systems for the same molecules.[18,19] To our knowledge, no experimental data exist to compare to any of these adsorption energies for the case of D_2. However, the value for graphite is in good agreement with the energies per particle for this registered structure given by Novaco.[20] The approximate 2% difference can be ascribed to the slightly different Lennard-Jones parameters used in that work.

In both the experimental and simulated phase diagrams of H_2 on graphite at high enough densities we have incommensurate triangular (IC) structures from $\rho > 0.08$ Å^{-2} up to the experimental density for the promotion to a second layer (0.093 Å^{-2}[26]). The experimental phase diagrams for D_2 on the same substrate[6,7,13–15] are similar to those of hydrogen in this aspect: they end up in triangular solids right before the second layer promotion at 0.099 Å^{-2}[26]. In Fig. 2 we represent the adsorption energy per particle of that IC phase on graphene (triangles and dashed line) together with that corresponding to a C solid (diamond) whose numerical value is given in Table II. The x axis of Fig. 2 is the inverse of the deuterium density since the stability limits of the different solid phases will be defined with the help of a double-tangent Maxwell construction for which a display of the energy per particle versus the inverse of the density is needed. We used graphene as representative of both graphene and graphite since, as indicated above and as can be seen in Table III, the main difference in the equation of state for these substances is an offset of ∼53 K in the binding energies per particle. From Fig. 2 we can also deduce that the $\sqrt{3} \times \sqrt{3}$ phase is the ground state of D_2 adsorbed on graphene since its energy per particle is the lowest for all arrangements displayed there.

Between the C and IC phases, H_2 on graphite conforms to a striped domain wall arrangement called α. This is also true for D_2 on the same substrate. Following Ref. 6, we modeled the α structure as a strip of a $\sqrt{3} \times \sqrt{3}$ solid of variable width limited by walls in which the distances between deuterium molecules

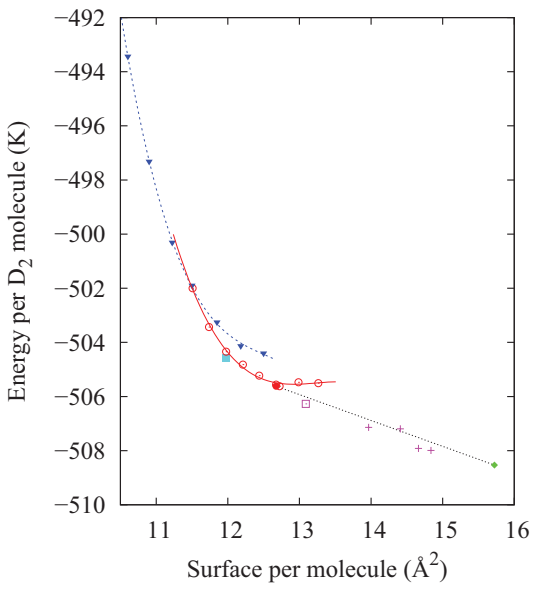

FIG. 2. (Color online) Energy per D_2 molecule (in K) for the different solid phases of deuterium on graphene. Diamond, $\sqrt{3} \times \sqrt{3}$ structure; open circles, γ phase; triangles, triangular incommensurate solid. The solid and dotted lines are least-squares fits of third-order polynomials to the simulation results represented as symbols. The solid square and solid circle indicate the ϵ and δ commensurate phases with the structures proposed in Ref. 6. The dotted line is the Maxwell double-tangent construction between the $\sqrt{3} \times \sqrt{3}$ and γ phases.

TABLE III. Densities ρ and energies per particle E (K) for each of the idealized structures that are supposed to be the building blocks of the striped domain phase. Both graphene and graphite values are shown.

Phase	ρ (Å^{-2})	E_{graphene} (K)	E_{graphite} (K)
α_4	0.0764	-506.27 ± 0.02	-559.19 ± 0.02
α_6	0.0716	-507.14 ± 0.03	-560.11 ± 0.03
α_8	0.0694	-507.21 ± 0.02	-560.25 ± 0.02
α_{10}	0.0682	-507.92 ± 0.01	-561.01 ± 0.01
α_{12}	0.0674	-507.99 ± 0.01	-561.16 ± 0.02

were smaller than in the C phase. An example is displayed in Fig. 3. There, the squares are the underlying carbon atoms on the graphene, and the irregular splotches are formed by the superposition of 300 sets of D_2 coordinates represented by a single cross each. The rectangle defines the unit cell at the particular density (0.0716 Å^{-2}) displayed there, one with dimensions of 19.67 × 4.26 Å^2. This structure is the one labeled α_6 in Table I. The index 6 comes from the number of deuterium molecules (or D_2 columns) inside the simulation cell. If instead of six we had eight particles (α_8), the length of the simulation cell would increase to 27.05 Å, leaving the width unchanged. Figure 3 corresponds to the simulation cell used in our calculations for an α_6 arrangement, whose dimensions are 39.34 × 38.33 Å^2 and which includes 108 D_2 molecules.

In Fig. 2, we display the energies per particle for the idealized structures α_n, with $n = 6,8,10,12$ as crosses. The theoretical density limit for this striped phase corresponds to an α_4 arrangement, the open square in Fig. 2. Those energies are given in Table III. One would expect the striped phase to be a mixture of several of these idealized α_n structures in the right proportions for each density. We should also bear in mind that when the walls are infinitely separated from each other, we should recover the energy per particle of the C phase. We have then a solid phase in the density range 0.0636–0.0764 Å^{-2}, with energies per particle that are the weighted averages of the ones in Table III for each density. Obviously, we do not know the particular values for these energies, but we are confident that they will be located below the dotted line (see below) in Fig. 2, as are virtually all the values for the idealized structures. This means that the α phase is stable with respect to a mixture of C and γ phases (see below). This is also true of D_2 on graphite. The experimental upper limit for this α phase on graphite is 0.0738 Å^{-2}, which is lower than the density of the α_4 structure. This is probably due to the small length of the unit cell of this arrangement(12.30 Å), which implies a very short distance between walls (9.84 Å), and that would penalize energetically any structure that contains this unit cell.

The dotted line in Fig. 2 is the Maxwell double tangent between the C and γ phases. Since the former structure is represented by a single density, we cannot in truth make a Maxwell construction between two curves, so the dotted line is the one with the smaller slope between the solid curve (a third-order polynomial fit to the simulation results indicated by open circles) and the single density of the registered $\sqrt{3} \times \sqrt{3}$ commensurate solid. The γ phase is an oblique arrangement defined by a rhomboid unit cell made up of two equilateral triangles joined on one side. This structure has been found experimentally only for D_2 on graphite and not for H_2 in the same substrate. A previous DMC calculation[9] for H_2 on graphene indicated that this arrangement was unstable with respect to a triangular incommensurate solid. An example of a typical unit cell is displayed in Fig. 4. There, the shortest distance between the molecules located at the opposite vertices of the rhomboid is the same as the side of the unit cell and equals 3.755 Å (corresponding to a density of 0.0819 Å^{-2}). To define the structure completely we need also the angle that the unit cell forms with the vertical axis, 10.2° in the case of Fig. 4. The rest of the data for the open circles in Fig. 2 was obtained by defining oblique simulation cells containing 12 × 12 rhomboids of the type displayed in Fig. 4 with the adequate side lengths to obtain the desired densities. The rotation angles varied linearly from 7.5° for 0.076 Å^{-2} to 12° for 0.086 Å^{-2}

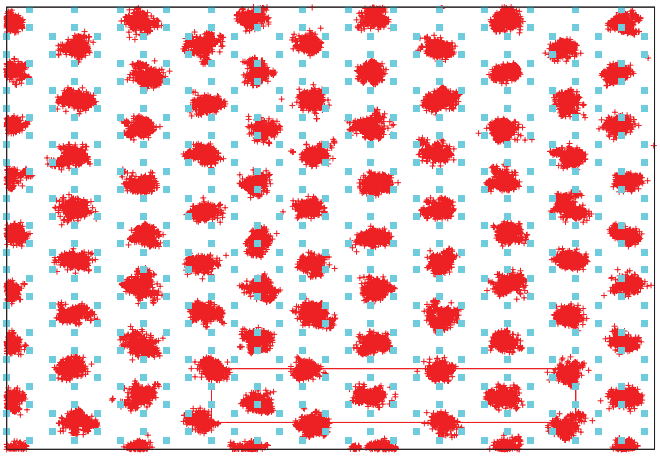

FIG. 3. (Color online) Simulation cell used for the α_6 structure, as defined in the text. The solid squares represent the carbon atoms of the underlying graphene sheet. Solid smudges are the result of displaying 300 sets of deuterium coordinates represented as crosses. The unit cell of this solid, containing six D_2 molecules, is displayed as a rectangle.

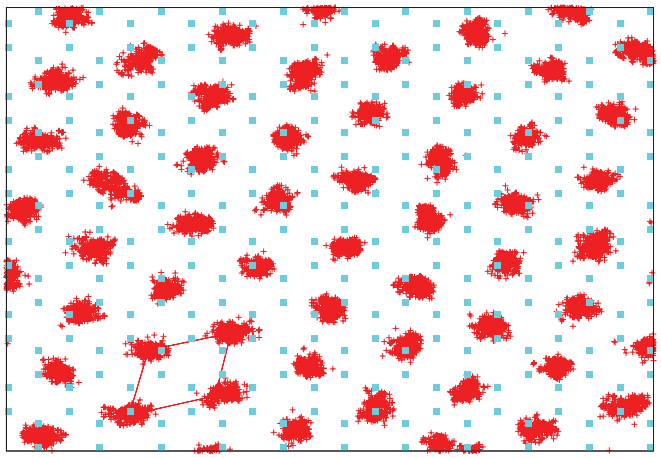

FIG. 4. (Color online) Depiction of the γ structure for a density of 0.0819 Å^{-2} and a rotation angle of 10.2°. The rhomboid is its unit cell. The symbols have the same meaning as in Fig. 3.

(experimental values from the low-energy electron diffraction (LEED) measurements in Ref. 14).

The Maxwell construction between the C phase and the γ phase ends up at $\sim$0.0789 Å^{-2} for both graphene and graphite (whose data are not shown for simplicity). This is the value corresponding to the δ commensurate structure inferred from calorimetric measurements and remains basically unchanged if instead of the C phase we used the theoretical limit of the α phase (open square in Fig. 2 for the double tangent). This means that at least between 0.0764 and 0.0789 Å^{-2} there is a coexistence zone between the α phase and the γ one. The differences in that lower limit and the experimental one (0.0738 Å^{-2}) have been already referred to above when we explained the implausibility of the α phase being extended up to the α_4 limit. The upper limit is within a $\sim$5% of the experimental value (0.0757 Å^{-2}[26]).

Another question is whether the δ and ϵ phases do really exist as these two commensurate arrangements show up only in the calorimetric data for D_2 (not H_2) on graphite.[7,13] Neither arrangement was found to be theoretically stable in the case of H_2 or for graphene or graphite.[9] Those structures are displayed in Figs. 5 and 6. The simulation cell for the δ solid includes 124 molecules on a 36.89 × 42.60 Å^2 cell and the one for the ϵ structure has 112 particles on a 39.35 × 34.08 Å^2 cell. Both simulation cells are rectangular. Those last numbers mean a density of 0.0835 Å^{-2} for the ϵ phase. The structures depicted correspond to the uniformly compressed arrangements proposed in Ref. 6, which have lower energies than their heavy-domain-wall counterparts proposed in that reference for the same densities. The corresponding unit cells for these commensurate solids are given by the diamond in Fig. 5 and the rhombus in Fig. 6. Both structures are commensurate because the vertices of their respective unit cells are adsorbed on the center of a carbon hexagon on the underlying graphene or graphite. However, as can be seen in Fig. 5, both solids can also be described with oblique unit cells similar to those of the γ phase. The only difference is that when the solids are built this way we have, in general, *incommensurate* arrangements. The energies per particle for all these structures are given in Table IV for both graphene and graphite. There, we can see that the δ structure and its γ counterpart are almost within each other's error bars, something that it is not true of the ϵ phase and its incommensurate partner. The energies for the δ and ϵ heavy-domain-wall structures are also given for comparison. All this means that the δ commensurate solid is virtually identical and can be considered as part of the γ phase, while the ϵ phase is different from the rotated oblique structure. This is due to the fact that in the δ phase the additional stabilization due to commensurability is caused by the location of one D_2 molecule per unit cell on the center of one carbon hexagon (the unit cell contains 31 molecules), while in the ϵ case, we have a commensurate contribution for one in every seven particles adsorbed on graphene and graphite (see Fig. 6). In any case, at least at $T = 0$ K, the molecule disposition and energy per particle between those pairs of structures are very small, which explains why it is difficult to distinguish them experimentally in the graphite case.

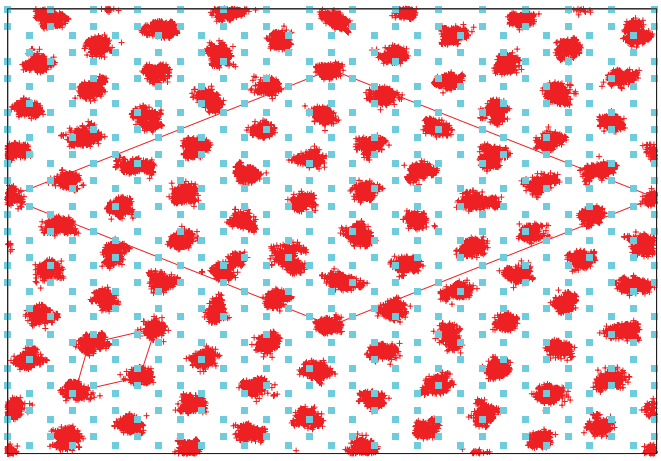

FIG. 5. (Color online) Sketch of the uniformly compressed δ structure as proposed in Ref. 6. The big diamond is the unit cell for this arrangement compared to the small rhomboid of a γ-like structure for the same density. The symbols have the same meaning as those of Fig. 3.

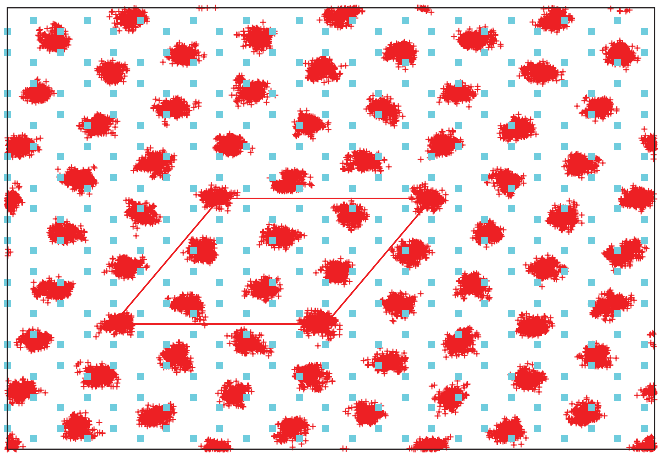

FIG. 6. (Color online) Same as in Fig. 5, but for the ϵ solid at 0.0839 Å^{-2}. The corresponding γ unit cell is not displayed for simplicity, but it can be readily deduced from the disposition of the D_2 smudges.

From the above discussion, we can consider that the stability range of the γ phase is between 0.0789 and 0.0835 Å^{-2}, with the second density corresponding to the ϵ phase. From that single point, we will have to perform another Maxwell construction to establish the next stable solid upon a pressure increase. If we try to draw the line with the minimum slope from the solid square in Fig. 2 up, we will find that it will end at a density of $\sim$0.0869 Å^{-2} (corresponding to the confluence of a triangle and an open circle). Since the open circle would be the end of the stability of the γ phase, this indicates that the ϵ solid is in equilibrium with a triangular incommensurate phase from that density on. Experimentally, it is known that for graphite this IC solid appears above 0.0840 Å^{-2}. This agrees with our results since above 0.0835 Å^{-2} and up to 0.0869 Å^{-2} (the limit of the double-tangent construction), we have a mixture of ϵ and IC solids. Even though this conclusion is reached for graphene, it holds also for graphite as well since the limits are similar to those of graphene.

TABLE IV. Energies per D_2 molecule for the different possible structures at the densities corresponding to the δ and ϵ arrangements.

Phase	ρ (Å^{-2})	E_{graphene} (K)	E_{graphite} (K)
δ (uniformly compressed)	0.0789	-505.62 ± 0.03	-558.19 ± 0.03
δ (heavy domain walls)	0.0789	-503.69 ± 0.03	-556.4 ± 0.1
γ	0.0789	-505.56 ± 0.02	-558.17 ± 0.02
ϵ (uniformly compressed)	0.0835	-504.57 ± 0.03	-557.12 ± 0.02
ϵ (heavy domain walls)	0.0835	-501.01 ± 0.05	-553.89 ± 0.07
γ	0.0835	-504.34 ± 0.03	-556.94 ± 0.02

IV. CONCLUSIONS

We have studied the phase diagrams of D_2 on graphene and graphite by means of the diffusion Monte Carlo technique. From the study of the unstable liquid phase, we concluded that virtually the only difference between those diagrams is an energy offset of ∼53 K per particle due to the greater number of graphene sheets present in graphite with respect to graphene. The main part of the graphite-deuterium interaction is due to the first two graphene layers, as can be seen from the data in Table II. We found also that the ground state for those structures is a $\sqrt{3} \times \sqrt{3}$ commensurate solid followed by a striped domain α solid and a γ structure with an oblique unit cell rotated with respect to the one of a triangular incommensurate phase. This last IC phase becomes stable at high enough densities. The δ arrangement was found to be barely distinguishable from its γ counterpart at the same density, something that it is not true of the ϵ commensurate arrangement. Since any of these three solids were seen in either the experimental or theoretical phase diagrams of H_2 on graphene or graphite, we can say that the description of the system afforded by our simulations is good enough to distinguish both isotopes, and it is able to reproduce the experimental phase diagram of D_2 on graphite at low temperatures.

ACKNOWLEDGMENTS

We acknowledge partial financial support from the Junta de de Andalucía Group PAI-205, Grant No. FQM-5985, and MICINN (Spain), Grant No. FIS2010-18356.

[1] L. W. Bruch, M. W. Cole, and E. Zaremba, *Physical Adsorption: Forces and Phenomena* (Oxford University Press, Oxford 1997).
[2] D. S. Greywall and P. A. Busch, Phys. Rev. Lett. **67**, 3535 (1991).
[3] D. S. Greywall, Phys. Rev. B **47**, 309 (1993).
[4] H. Freimuth and H. Wiechert., Surf. Sci. **162**, 432 (1985).
[5] H. Freimuth, H. Wiechert, and H. J. Lauter, Surf. Sci. **189-190**, 548 (1987).
[6] H. Freimuth, H. Wiechert, H. P. Schildberg, and H. J. Lauter, Phys. Rev. B. **42**, 587 (1990).
[7] H. Wiechert, Phys. B **169**, 144 (1991).
[8] M. C. Gordillo and J. Boronat, Phys. Rev. Lett. **102**, 085303 (2009).
[9] M. C. Gordillo and J. Boronat, Phys. Rev. B **81**, 155435 (2010).
[10] K. S. Novoselov, A. K. Geim, S. V. Morozov, D. Jiang, Y. Zhang, S. V. Dubonos, I. V. Grigorieva, and A. A. Firsov, Science **306**, 666 (2004).
[11] K. S. Novoselov, D. Jiang, F. Schedin, T. J. Booth, V. V. Khotkevich, S. V. Morozov, and A. K. Geim, Proc. Natl. Acad. Sci. USA **102**, 10451 (2005).
[12] C. H. Lui, L. Liu, K. F. Mak, G. W. Flynn, and T. F. Heinz, Nature (London) **462**, 339 (2009).
[13] H. Freimuth and H. Wiechert, Surf. Sci. **178**, 716 (1986).
[14] J. Cui, S. C. Fain Jr., H. Freimuth, H. Wiechert, H. P. Schildberg, and H. J. Lauter, Phys. Rev. Lett. **60**, 1848 (1988).
[15] J. Cui and S. C. Fain Jr., Phys. Rev. B **39**, 8628 (1989).
[16] J. Boronat and J. Casulleras, Phys. Rev. B **49**, 8920 (1994).
[17] G. Stan and M. W. Cole, J. Low Temp. Phys. **110**, 539 (1998).
[18] M. C. Gordillo, J. Boronat, and J. Casulleras, Phys. Rev. B **65**, 014503 (2001).
[19] M. C. Gordillo, J. Boronat, and J. Casulleras, Phys. Rev. B **68**, 125421 (2003).
[20] A. D. Novaco, Phys. Rev. B **46**, 8178 (1992).
[21] C. Cazorla and J. Boronat, Phys. Rev. B **78**, 134509 (2008).
[22] I. F. Silvera and V. V. Goldman, J. Chem. Phys. **69**, 4209 (1978).